Carbohydrate Polymers 121 (2015) 276–283

Contents lists available at ScienceDirect

Carbohydrate Polymers

journal homepage: www.elsevier.com/locate/carbpol

Controlled uptake and release of lysozyme from glycerol diglycidyl ether cross-linked oxidized starch microgel

Luhai Zhao, Yuying Chen, Wei Li, Meiling Lu, Shanshan Wang, Xiaodong Chen, Mengxuan Shi, Jiande Wu, Qipeng Yuan, Yuan Li *

State Key Laboratory of Chemical Resource Engineering, Beijing University of Chemical Technology, College of Life Science and Technology, P. O. Box 53, 100029 Beijing, China

ARTICLE INFO

Article history:
Received 3 October 2014
Received in revised form 1 January 2015
Accepted 3 January 2015
Available online 7 January 2015

Keywords:
Oxidized starch microgels
Protein absorption
Lysozyme
pH responsive
Controlled release
TEMPO-oxidation

ABSTRACT

A biodegradable microgel system based on glycerol-1,3-diglycidyl ether (GDGE) cross-linked TEMPO-oxidized potato starch polymers was developed for controlled uptake and release of proteins. A series of microgels were prepared with a wide range of charge density and cross-link density. We found both swelling capacity (SW_w) and lysozyme uptake at saturation (Γ_{sat}) increased with increasing degree of oxidation (DO) and decreasing cross-link density. Microgel of DO100% with a low cross-link density ($R_{GDGE/polymer\,(w/w)}$ of 0.025) was selected to be the optimum gel type for lysozyme absorption; Γ_{sat} increased with increasing pH and decreasing ionic strength. It suggests that the binding strength was the strongest at high pH and low ionic strength, which was recognized as the optimum absorption conditions. The lysozyme release was promoted at low pH and high ionic strength, which were considered to be the most suitable conditions for triggering protein release. These results may provide useful information for the controlled uptake and release of proteins by oxidized starch microgels.

1. Introduction

Microgels have been of great interest to scientists in the past few decades because of their favorable biocompatible properties and sensitivity to external stimuli, such as temperature (Drapala et al., 2014), pH (Koetting & Peppas, 2014), light (Schesny et al., 2014), ionic strength (Li, Norde, & Kleijn, 2012), and applied electric or magnetic fields (Bardajee & Hooshyar, 2013; Gonzalez et al., 2014; Guilherme et al., 2012). Microgels can be applied in tissue repairing (Lau & Wang, 2013), drug delivery systems (Singh, Bala, & Chauhan, 2008), biosensors (Liu et al., 2015), chromatography (Qu et al., 2014) and medical devices (Li et al., 2014). The three-dimensional network of microgels allows a controlled uptake and release of functional ingredients, bioactive compounds and drugs for various purposes (Lynam et al., 2014).

Both synthetic polymers, such as poly(acrylic acid) (PAA) (Bysell & Malmsten, 2006), poly(ether-urethane) (PEU) (Li et al., 2014), poly(ethylene glycol) (PEG) (Tomic, Veeman, Boerakker, Litvinov, & Dias, 2008) and natural polymers, such as DNA (Costa, Valente, Pais, Miguel, & Lindman, 2010), chitosan (Zamora-Mora, Velasco, Hernandez, Mijangos, & Kumacheva, 2014), starch (Mehyar, Liu, & Han, 2008), cellulose (Grznarova, Yu, Stefuca, & Polakovic, 2005; Spagnol et al., 2012), hyaluronic acid (Widjaja et al., 2014), dextran (Imren, Gümüsderelioglu, & Güner, 2010), and Konjac glucomannan (Chen et al., 2014; Shahbuddin, MacNeil, & Rimmer, 2012), can be employed to prepare functional microgels. Microgels based on natural polymers have attracted considerable attention in biomedical applications because of their biocompatibility and biodegradability (Li et al., 2009). In order to protect the active components and release them at the targeted place where required, the development of effective encapsulation systems consisting of natural polymers has become an important issue.

Previously, we have developed a microgel carrier system based on TEMPO-oxidized potato starch. It is a microgel system consisting of a sodium trimetaphosphate (STMP) cross-linked oxidized starch polymer (Li et al., 2010, 2009). These microgels have unique advantages such as well-controlled charge density and cross-linking density. Since these microgels are sensitive to external conditions, e.g., ionic strength and pH, the absorption and release of active components inside the gels can be controlled by environmental conditions. The negatively charged starch microgel can absorb positively charged functional ingredients such as proteins (Li et al., 2011a, 2011b) and anthocyanins (Wang, Li, Chen, Xin, & Yuan, 2013) through electrostatic interactions. Additionally, release of the active ingredients can be triggered under certain conditions, e.g., high pH, high salt concentrations and enzymatic attack (Li

* Corresponding author. Tel.: +86 10 64447747; fax: +86 10 64416428.
E-mail address: liyuan@mail.buct.edu.cn (Y. Li).

http://dx.doi.org/10.1016/j.carbpol.2015.01.002
0144-8617/

et al., 2011a, 2011b). In this study, we developed a new microgel system based on glycerol diglycidyl ether (GDGE) cross-linked oxidized starch polymers. A series of microgels with a wide range of charge density and cross-link density were prepared.

Many drugs are proteins or polypeptides, such as insulin, and they may be degraded by proteases in the body before they arrive at the target site (Hosseininasab et al., 2014). Therefore, such proteins need a carrier system to protect them and deliver them to the targeted areas. We chose lysozyme as a model protein to study its uptake and release behavior in GDGE cross-linked starch microgels. Positively charged lysozyme can be absorbed by negatively charged starch microgels via electrostatic interactions. The pH and ionic strength may greatly affect protein absorption on a microgel by tuning the electrostatic interaction between them. Many studies have focused on the protein absorption capacity as a function of pH and ionic strength in order to determine the optimum absorption conditions. Cai, Bakowsky, Rytting, Schaper, and Kissel (2008) found that increased pH facilitated the adsorption of lysozyme by poly(lactide-co-glycolide) (PLGA) microspheres. Loading efficiency decreased with increasing ionic strength above the optimum salt concentration of 50 mM.

In this study, we first characterized the microgels with respect to their surface morphology, size distribution and swelling capacity. Next, the protein uptake capacity was measured as a function of the charge density and cross-link density, with the aim of selecting the optimal gels for encapsulation applications. Then, the protein uptake capacity was examined as a function of pH and ionic strength, in order to determine the optimum absorption conditions. Finally, the percentage of protein release was investigated at various pH levels and ionic strengths to assess the release behavior upon different conditions. The influence of these factors on protein uptake and release provided us with useful information for applying these microgel systems in biomedical applications.

2. Materials and methods

2.1. Materials

Potato starch polymer was kindly offered by AVEBE, The Netherlands. The oxidation catalyst 2,2,6,6-tetramethyl-1-piperidinyloxy (TEMPO) and the globular protein lysozyme (from chicken egg white, Mw = 14,400 g/mol, activity>20,000 μm/mg) were obtained from Sigma–Aldrich, USA. The cross-linking agent glycerol-1,3-diglycidyl ether (GDGE) was provided by Amresco, USA. Purified Milli-Q water was used throughout. All other chemicals used were of analytical grade.

2.2. Methods

2.2.1. The preparation of oxidized starch microgel

The primary alcohol groups at the C-6 position on potato starch polymer were selectively oxidized into carboxyl groups by TEMPO-mediated oxidation. In this way, the oxidized starch of various degree of oxidation (DO) 30%, 50%, 70%, 100% were prepared, following the procedure developed by de Nooy (1997). The DO was controlled by the amount of sodium hypochlorite added during oxidation. The accurate DO was determined in our previous study by proton titration method (Li et al., 2009).

Microgel were prepared by cross-linking the oxidized starch polymer with GDGE at pH 10. According to literature, diepoxy GDGE are more likely to react with carboxyl groups under basic condition than the hydroxyl groups on polymer (Fleisher & Vigh, 2005). So that in our case, most likely that major carboxyl groups and minor hydroxyl groups participated in the cross-link reaction. GDGE forms intermolecular linkage between two different starch polymers. First, 12 g potato starch polymers were dissolved in 80 mL distilled water at room temperature. Then 1 M NaOH was added into the polymer solution to adjust the pH into pH 10. Thereafter, the cross-linker GDGE was added into the polymer solution and the mixture was heated at 40 °C for 10 min. Then the preformed hydrogels were put in an oven at 40 °C for 72 h for further cross-linking. The weight ratio of cross-linker to starch polymer ($R_{cross\text{-}linker/polymer}$) were 0.025, 0.04, 0.05, and 0.065. After the hydrogels were formed, the whole piece of gel was grinded, and the grinded gel pieces were passed through a sieve (mesh size: 1 mm) covered with a nylon cloth of 200 mesh (mesh size: 0.074 mm), in order to obtain reasonably uniform microgel particles. The gel particles were washed three times with distilled water using the nylon covered above a sieve again to remove the salts. Thereafter, the hydrogel particles were washed three times again with 100% ethanol to remove water and three times with 100% acetone to wash out ethanol and last traces of water. Finally, the hydrogel particles were dried in oven at 40 °C overnight. The dried microgel powder was again grinded by a glass mortar to achieve small and homogenous particles.

2.2.2. The size distribution of microgel particles

The size distribution of microgel particle in aqueous suspension was measured using a Malvern Mastersizer 2000 (Malvern, UK). In the laser diffraction measurement, particles pass through the focused laser beam and scattered light at an angle that is inversely proportional to their diameter. A dual wavelength detection system (blue light combined with red light) was used to promote detective performance and sensitivity. Before the measurements, the microgel powder was dissolved in distilled water for at least 4 h to allow equilibrium. Then the gel suspensions were sonicated for 10 min to get finely dispersed gel particles. The gel particles were diluted 1:100 to avoid multiple scattering effects. Gel particles diameter was estimated by the average of three measurements.

2.2.3. Scanning electron microscopy

The surface morphology of microgel particles was examined by scanning electron microscopy (SEM) using SEM (S-4700, Hitachi Company, Japan) with an accelerating voltage of 15 kV. Microgel particles were freeze dried by lyophilizing under vacuum (Dura-Dry TMMP, USA). Then microgel particles were sputter-coated with gold prior to observation.

2.2.4. Weight swelling capacity (FSC) measurements

A known weight of dried microgel powder (around 0.01 g) was immersed in an excess of distilled water to equilibrium swelling at room temperature. The swollen microgels of various DO and cross-link densities were immersed in the distilled water for 2 h to reach equilibrium. Then the excess water was wiped off with papers until there were no visible water droplets, and the swollen gel cannot flow freely. Swelling ratio (SW_w) is defined as the weight ratio of the swollen gel to the dried gel:

$$SW_w = \frac{W_{\text{swollen-gel}}}{W_{\text{dry-gel}}} \quad (1)$$

2.2.5. Zeta potential measurements

Zeta potential of microgel particles in buffer of various pH and ionic strength was determined using a Malvern Nanosizer ZS2000 (Malvern, UK). The instrument measures the direction and velocity of a macromolecule or particle in an applied electrical field via phase analysis light scattering and laser Doppler velocimetry. The calculated electrophoretic mobility is converted into zeta potential values using the Smoluchowski model. The temperature of all samples was controlled at 25 °C. Before the measurements, the microgel suspensions were sonicated for 15 min, in order to attain

finely dispersed gel particles. After loading the samples into the instrument they were equilibrated for about 120 s. The data were averaged over 20 continuous measurements.

2.2.6. Protein absorption isotherm

Before the measurements, microgels were sonicated for 10 min, in order to obtain finely dispersed gel particles. The uptake of lysozyme into microgel particles was studied by mixing gel suspension with solutions of increasing lysozyme concentration if steps of 1 mL with 10 min delay time after each step. The absorption of lysozyme in the microgel will become saturated after a certain time. 1 mL lysozyme solution (6.67 g/L) was added into 10 mL microgel suspension (2 g/L) while stirring. After 10 min loading time, 1 mL of the mixture solution was sampled, and another 1 mL lysozyme solution was added while continually stirring for 10 min. This was repeated for another 9 times. Finally, all the samples were centrifuged under 10,000 rpm for 5 min, and the concentration of lysozyme in the supernatants was measured by absorbance at wavelength 280 nm determined with UV spectrophotometer. The uptake (mg lysozyme/mg of dry gel) of lysozyme in the hydrogel particles was calculated from material balance. At a gel concentration of 2 g/L, the volume of the swollen gel is less than 5% of the total volume. This volume fraction was neglected when calculating lysozyme uptake. The absorption isotherm was attained by plotting the amount of the lysozyme absorbed by the microgel against the equilibrium lysozyme concentration in solution.

2.2.7. Protein uptake capacity at saturation

3 mg of dry gel particles were suspended in 5 mL buffer of various pH and ionic strength for at least 4 h equilibrium. Then 5 mL of 10 g/L lysozyme solution were added into the gel, and gently stirred under a magnetic stirrer for 5 h (sufficient time to reach saturation) for reaching the maximum protein uptake. Subsequently, the microgel-protein mixtures were centrifuged at 10,000 rpm for 5 min, and the concentration of unabsorbed lysozyme in the supernatant was determined by UV spectrophotometry at 280 nm. The total protein adsorption at saturation level Γ_{sat} (g protein/g dry gel) in the hydrogel particles was calculated from the mass balance. After centrifugation, the supernatant was removed and the microgel-protein complexes were subsequently vacuum-freeze dried. The freeze-dried lysozyme-microgel complexes were further used for the release study.

2.2.8. In vitro release of lysozyme from oxidized starch microgel

The dried microgel-lysozyme complexes were re-dissolved in 10 mL buffer of various pH and ionic strength under mildly stirring. At scheduled time intervals, the samples were taken up and centrifuged (10,000 rpm, 5 min). The amount of protein released can be calculated form the absorbance of the supernatant at 280 nm. The protein release from the gel was compared at different pH and ionic strength. The citric acids-phosphate buffers were used to achieve pH of the 3, 4, 5 and 7 at a fixed ionic strength of 0.05 M, and ionic strength of 0.05, 0.2 and 0.5 M at a fixed pH of pH 7. The percentage of protein released $P_{release}$ is calculated from the measured protein concentration C_{prot} in supernatant as:

$$P_{release} = \frac{C_{prot} \times 10\,mL}{\Gamma_{sat} \times m_{dry\ gel}} \times 100\% \quad (2)$$

C_{prot} (g/L) is the protein concentration in the supernatant during the release experiment. Γ_{sat} (g protein/g dry gel) is the protein uptake capacity at saturation. $m_{dry\ gel}$ (g) is the weight of the dry gel particles used in release experiment.

All experiments (absorption and release) were repeated at least three times. The results are reported are average values.

3. Results and discussion

3.1. Characterization of oxidized starch microgels

As shown in Fig. 1, the oxidized starch microgels (after sonification) had a relatively broad size distribution, ranging between 1 and 100 μm, although most particles were distributed between 10 and 20 μm. The average diameter for DO30 with a weight ratio between GDGE and the polymer ($R_{GDGE/polymer(w/w)}$) of 0.025 was 21 μm; DO100 with a $R_{GDGE/polymer(w/w)}$ of 0.025 had an average diameter of 20.9 μm and DO100 with a $R_{GDGE/polymer(w/w)}$ of 0.065 had an average diameter of 18.4 μm. It seems that the size distribution did not vary much among microgels of different DO and cross-link density.

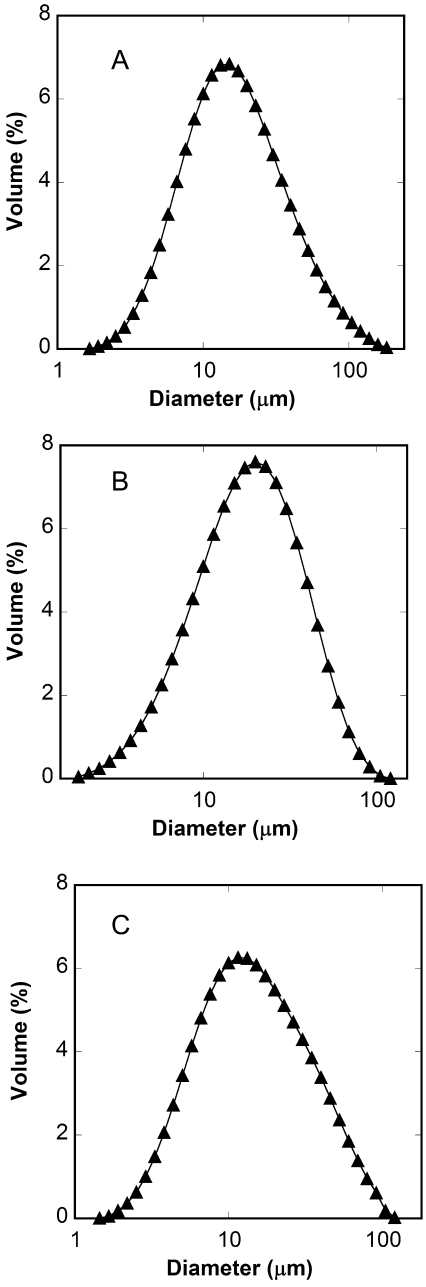

Fig. 1. Size distribution of oxidized starch microgels (A) DO30%, $R_{GDGE/polymer\,(w/w)}$ of 0.025; (B) DO100%, $R_{GDGE/polymer\,(w/w)}$ of 0.025; (C) DO100%, $R_{GDGE/polymer\,(w/w)}$ of 0.065.

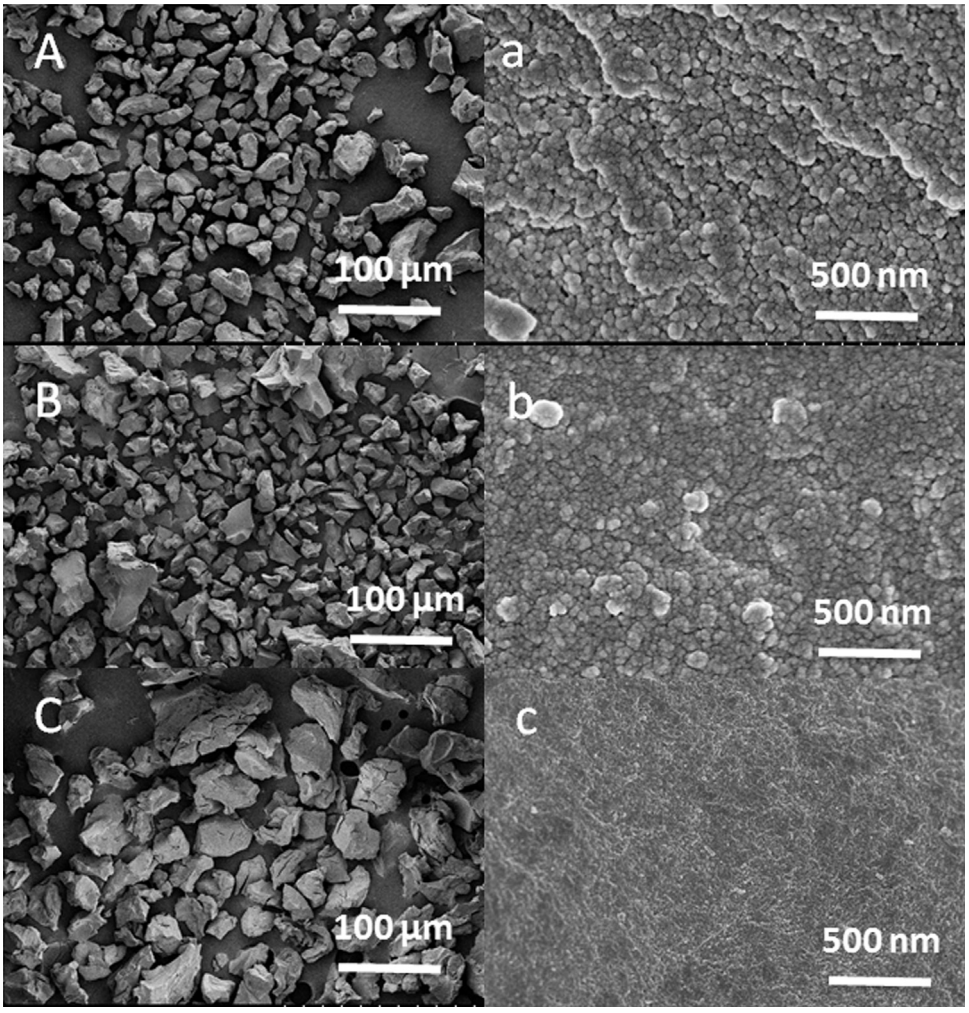

Fig. 2. SEM photographs of oxidized starch microgels. (A) Particle morphology of DO100%, $R_{GDGE/polymer\ (w/w)}$ of 0.025, (a) magnified image on the particle surface; (B) particle morphology of DO100%, $R_{GDGE/polymer\ (w/w)}$ of 0.065, (b) magnified image on the particle surface; (C) particle morphology of DO30%, $R_{GDGE/polymer\ (w/w)}$ of 0.025, (c) magnified image on the particle surface.

The surface morphology of oxidized starch microgels were characterized by scanning electron microscopy (Fig. 2). The microgel particles present similar appearance for all microgels (Fig. 2A–C). It was found that, for microgels of the same cross-link density $R_{GDGE/polymer(w/w)}$ of 0.025, the DO100 microgel (Fig. 2a) had larger surface pores than the DO30 microgel (Fig. 2c). For microgels of same DO–DO100, microgels with a lower cross-link density $R_{GDGE/polymer(w/w)}$ of 0.025 (Fig. 2a) had larger surface pores than microgels with a higher cross-link density $R_{GDGE/polymer(w/w)}$ of 0.065 (Fig. 2b). The surface pores may relate to its swelling capacity and protein uptake capacity.

A polymer network immersed in a good solvent imbibes the solvent in order to balance the solvent chemical potential inside and outside the gel network; the presence of cross-links restricts the extent of swelling. Thus, swelling continues until the sum of the elastic forces between cross-links is equal to the osmotic force (Saunders & Vincent, 1999). Swelling capacity is an important physical chemical property for microgel. The swelling capacities of oxidized starch microgels were investigated as a function of the DO and cross-link density ($R_{GDGE/polymer\ (w/w)}$) in distilled water (pH 7) at room temperature. As shown in Fig. 3, the weight swelling ratio (SW_w) increased with increasing DO and decreased with increasing cross-link density ($R_{GDGE/polymer\ (w/w)}$). This swelling behavior may be related to the mechanism of the cross-linking reaction between glycerol-1,3-diglycidyl ether (GDGE) and the oxidized starch polymers. According to the literature, the carboxyl and hydroxyl groups on the polymer chain can work as nucleophilic agents and attack the carbon atom of the epoxide group on GDGE, forming an ester or ether to cross-link the polymers together. Diepoxy GDGE are more likely to react with carboxyl groups under basic conditions than hydroxyl groups (Fleisher & Vigh, 2005). So that in our case, it is most likely that major carboxyl groups and minor

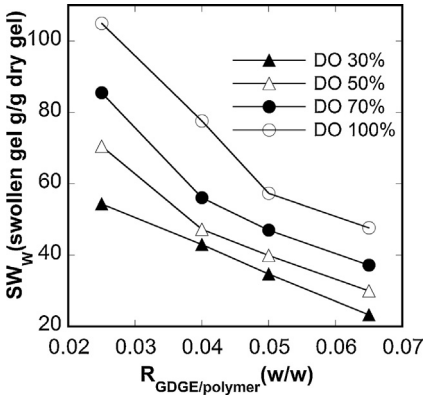

Fig. 3. Weight swelling ratio SW_w (swollen gel g/g dried gel) vs. cross-link density ($R_{GDGE/polymer\ (w/w)}$) for microgel of various degree of oxidation (DO).

hydroxyl groups participated in the cross-linking reaction. It was expected that microgels with a higher DO would have a greater swelling capacity. Even though some of the COO^- groups take part in the cross-linking reaction, there are still a considerable number of COO^- groups remaining on the polymer. The microgels with higher DO possess many more carboxyl groups, which dissociate at pH 7, leading to a microgel with a high negative charge and, hence, leading to repulsion between the polymers. The electrostatic repulsion between oxidized starch polymers may contribute to extra swelling of the gel network. It is expected that hydrogels made of charged polyelectrolytes have a much greater swelling capacity than hydrogels composed of neutral polymers. This is may be due to increased internal osmotic pressure because of the counter-ions contained within the charged microgels. In the present study, it was found that the swelling capacity decreased with increasing cross-link density for all microgels because the swelling of the hydrogel is restricted by increasing elasticity of the gel network due to increasing cross-link density. It has also been reported that the swelling of poly(methacrylic acid-co-acrylic acid) microgels decreases linearly when the molar fraction of the cross-linking monomer is increased (Lack et al., 2004). Besides, it seems that the surface pores of microgels increased with increasing swelling capacity, as Fig. 2 already showed that the microgels of higher DO (higher SW_w) had bigger pores, and microgels of higher cross-link density (lower SW_w) had smaller pores. The cross-linking mechanism of GDGE cross-link microgels differs from the oxidized starch microgels cross-linked with STMP. STMP reacted with two hydroxyl groups belonging to two different polymer chains. SW_w of STMP-microgels increased with increasing DO because COO^- groups did not participate into the cross-link reaction. Besides, we found that STMP cross-linked starch microgels possessed a critical cross-linker to polymer weight ratio above which the swelling of the gel do not change anymore (Li et al., 2009). This is because excess STMP over the critical amount of STMP cannot take part in the cross-link reaction anymore. Since the critical cross-link density has not yet appeared for GDGE cross-linked microgels, so that it suggests the cross-linkers used for GDGE-microgels have all participated in the cross-link reaction.

The surface charges of a microgel play a crucial role in electrostatic interactions with oppositely charged ingredients; they are also greatly influenced by the pH and ionic strength. The zeta-potential of the microgel was determined as a function of pH and ionic strength in order to determine the surface charge variation by changing the pH and ionic strength. As shown in Fig. 4A, the zeta-potential of the starch microgel decreased with increasing pH and reached a plateau value from pH 6 to 7 due to the dissociation of COO^- groups which increased with increasing pH; this was maximal at around pH 6. As shown in Fig. 4B, the zeta-potential of the starch microgel increased with increasing ionic strength at pH 7. This was ascribed to the shielding of the surface charges on the microgel by salt ions. It was expected that the surface charge on the gel would be the highest at high pH and low salt concentration. The trend of zeta-potential of GDGE cross-linked microgel as a function of pH and ionic strength was consistent with our previous finding on STMP cross-linked starch (Li et al., 2009). This may be due to that the surface charge will not vary among the starch gels cross-linked with different cross-linkers.

3.2. Protein absorption by oxidized starch microgels

The protein absorption isotherm was determined by measuring lysozyme uptake Γ (g protein/g dry gel) as a function of the protein concentration in solution C_{prot} (g/L) at equilibrium. The protein absorption experiments were performed using microgels of various DO at pH 7 and an ionic strength of 0.05 M. Lysozyme carries positive charges at pH 7 (the isoelectric point of lysozyme is pH 11), as shown in Fig. 4A, which can electrostatically interact with the negatively charged microgel (pK_a = pH 3.5, Li et al., 2009). As shown in Fig. 5, the initial part of the curve for Γ (g protein/g dry gel) rises steeply, which indicates that lysozyme absorbed with high affinity at low protein concentrations. The slope, reflecting the binding affinity, increased with increasing DO. The uptake increased and almost reached a plateau value when the lysozyme concentration was above 0.2–1 g/L. The plateau value reflects the maximal protein absorption capacity of the microgel, which is denoted as protein uptake at saturation, Γ_{sat} (g protein/g dry gel). The protein uptake

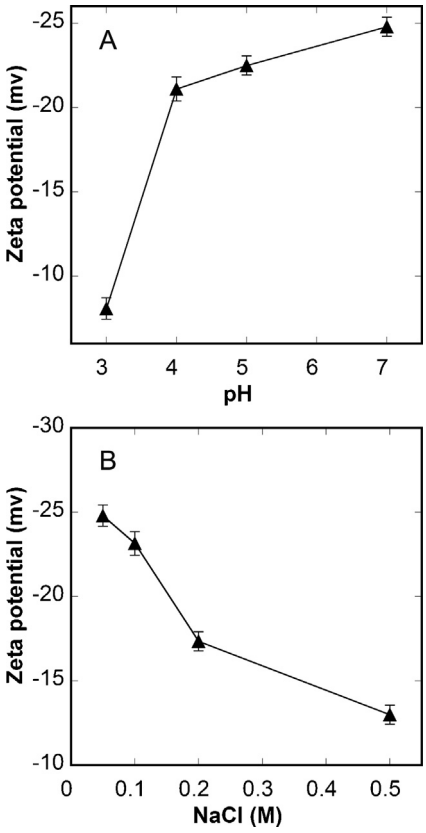

Fig. 4. Zeta-potential of DO100% microgel ($R_{GDGE/polymer\ (w/w)}$ of 0.025) as a function of (A) pH at a fixed ionic strength of 0.05 M and (B) ionic strength at a fixed pH of pH 7.

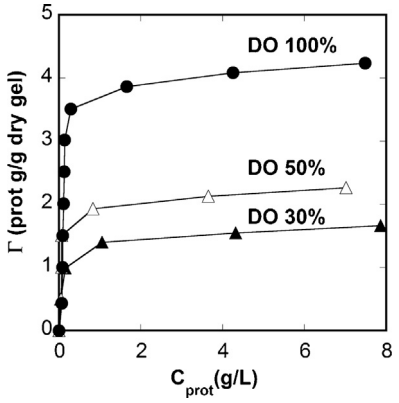

Fig. 5. Protein absorption isotherm: lysozyme uptake Γ (g protein/g dry gel) as a function of protein concentration in solution C_{prot} (g/L) at equilibrium. Buffer condition: pH 7 citric acid-phosphate buffer, ionic strength 0.05 M. For microgels of various degree of oxidation (DO30%, DO50%, DO70%, DO100%) with same cross-link density $R_{GDGE/polymer\ (w/w)}$ of 0.025.

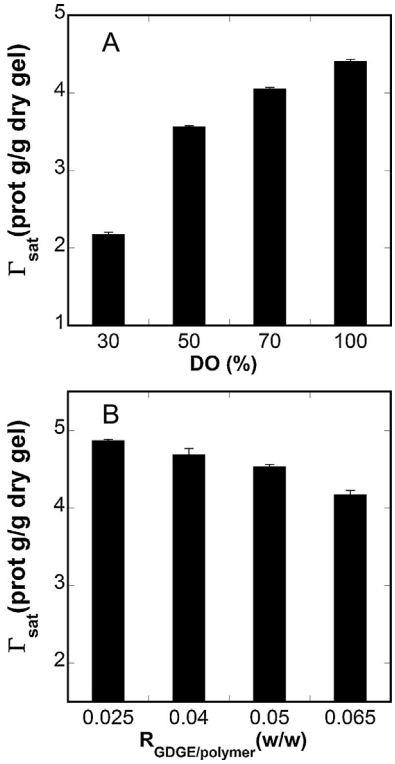

Fig. 6. (A) Protein uptake at saturation Γ_{sat} (g protein/g dry gel) for microgels of different degree of oxidation (DO30%, DO50%, DO70%, DO100%) with same cross-link density $R_{GDGE/polymer\ (w/w)}$ of 0.04. (B) Protein uptake at saturation Γ_{sat} (g protein/g dry gel) for DO100% microgels of different cross-link density ($R_{GDGE/polymer\ (w/w)}$: 0.025, 0.04, 0.05, 0.065). Buffer conditions for (A) and (B): pH 7 citric acid-phosphate buffer, ionic strength 0.05 M.

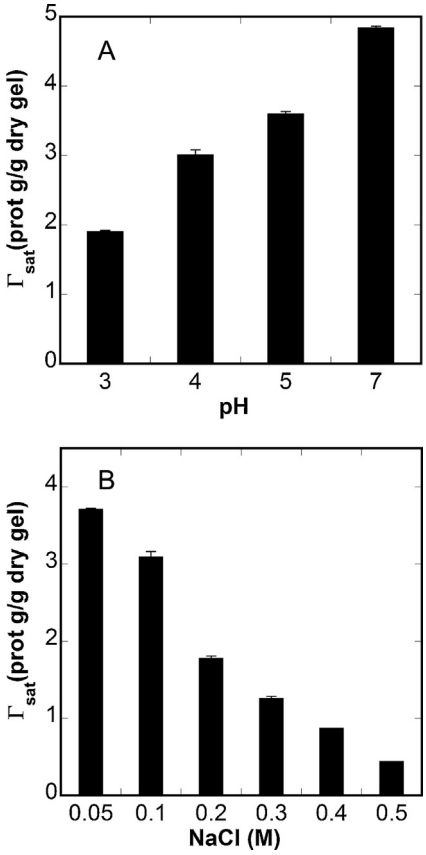

Fig. 7. Protein uptake at saturation Γ_{sat} (g protein/g dry gel) for DO100% microgels ($R_{GDGE/polymer\ (w/w)}$ of 0.025) as a function of (A) pH at a fixed ionic strength of 0.05 M and (B) ionic strength (M) at a fixed pH of pH 7. Citric acid-phosphate buffers were used.

at saturation increased with increasing DO, i.e. with increasing negative charge density in the gel, which increases the strength of the interaction between the microgel and lysozyme. For oxidized starch microgels cross-linked with STMP, we also find Γ_{sat} increases with increasing DO.

As indicated in Fig. 5, the protein uptake at saturation Γ_{sat} can be obtained from the plateau value of the protein absorption isotherm. It was known from the protein absorption isotherm experiment (Fig. 5) that 4 h of absorption time was sufficient for the microgel to reach saturation during protein absorption. Therefore, the protein uptake at saturation Γ_{sat} can be directly acquired from protein absorption after 4 h equilibrium. In this way, the protein uptake at saturation Γ_{sat} was measured as a function of DO and cross-link density. As shown in Fig. 6A, Γ_{sat} increased with increasing DO due to the increasing charge density on the microgel. As shown in Fig. 6B, for a microgel of a given charge density DO100%, the protein uptake at saturation Γ_{sat} decreased with increasing cross-link density ($R_{GDGE/polymer\ (w/w)}$). Γ_{sat} may be related to the swelling capacity and pore size of the microgel. We previously found that the swelling capacity (Fig. 3) and the pore size (Fig. 2) of a microgel also decrease with increasing cross-link density. The trend of protein uptake as a function of DO and cross-link density was consistent with our previous study on STMP cross-linked starch microgel (Li et al., 2009). It has been reported that the pore size of a microgel decreases with decreasing swelling capacity (Eichenbaum, Kiser, Dobrynin, Simon, & Needham, 1999) and, in turn, hinders the entry of protein molecules into the microgel. Therefore, the protein uptake is reduced. It can be concluded from the above results that the DO100% microgel with a lower cross-link density ($R_{GDGE/polymer\ (w/w)} = 0.025$) was the optimal microgel type for lysozyme uptake.

The optimal microgel type for lysozyme uptake (DO100% with a lower cross-link density $R_{GDGE/polymer\ (w/w)} = 0.025$) was applied to measure the optimum absorption conditions. The protein uptake at saturation Γ_{sat} was determined as a function of pH and ionic strength. As shown in Fig. 7A, Γ_{sat} increased with increasing pH at an ionic strength of 0.05 M. Fig. 4A already showed that the zeta-potential of unloaded microgel decreased at higher pH values due to the increasing dissociation of carboxyl groups from the microgel. The resulting increase in negative charge density on the microgel surface at elevated pH supplied more binding sites for positively charged proteins. However, the net positive charge of lysozyme decreases at higher pH, suggesting that more proteins are required to neutralize the increased negative charges on the gel. Therefore, protein absorption may increase in such a case. For oxidized starch microgel cross-linked with STMP, we find that the pH dependence on Γ_{sat} is further influenced by salt concentration. The curve of Γ_{sat} vs. pH for STMP cross-linked microgel showed a monotonic increase at low ionic strength (0.05 M), and this is consistent with that of GDGE cross-linked microgel. But for intermediate ionic strength (0.10 and 0.20 M), Γ_{sat} had a maximum at certain pH, denoted as pH_{opt}, and it shifted to lower pH with increasing ionic strength. This is because with increasing salt concentration, the screening effect is dominant, charge compensation becomes less important, and this leads to a decrease in protein uptake capacity Γ_{sat} at high pH (Li et al., 2010). This may provide a reference for the behavior of Γ_{sat} vs. pH for GDGE cross-linked microgels at intermediate ionic strength. Fig. 7B shows that Γ_{sat} decreased with an increasing salt concentration. This was due to the fact that salt shields charges on both the microgel (Fig. 4B) and proteins, leading to weakened electrostatic interactions and,

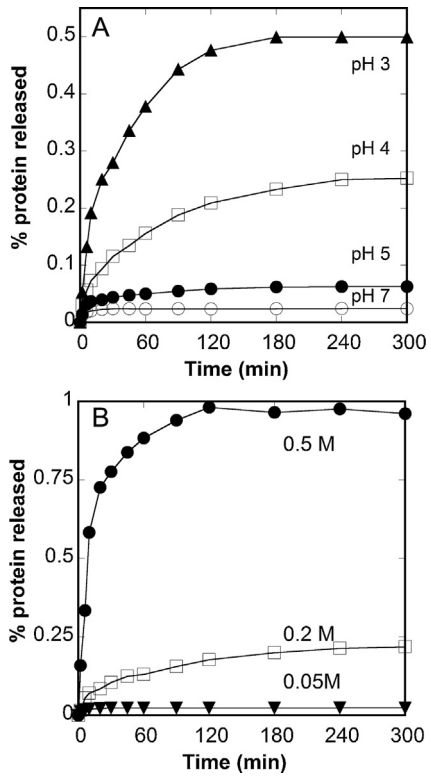

Fig. 8. Percentage of lysozyme release from DO100% microgel ($R_{GDGE/polymer\,(w/w)}$ of 0.025) at different time intervals (min) as a function of (A) pH at a fixed ionic strength of 0.05 M and (B) ionic strength (M) at a fixed pH of pH 7. Citric acid-phosphate buffers were used.

hence, reduced protein absorption. It can be concluded that pH 7 and an ionic strength of 0.05 M were the optimum protein absorption conditions. It has been previously reported that an increase in ionic strength could decrease protein absorption on a microgel due to the shielding effect on electrostatic forces, in cases where electrostatic interaction is the dominant driving force for protein absorption on a microgel (Li et al., 2010).

3.3. Protein release from oxidized starch microgels

In order to know the release behavior of lysozyme under various conditions, lysozyme molecules were first absorbed on starch microgels under the optimum conditions (pH 7, ionic strength 0.05 M) to achieve maximal protein absorption. Then, the microgel-protein complex was separated from unabsorbed proteins by centrifugation. Buffers of various conditions were added to the microgel-protein complex to trigger protein release. The percentage of lysozyme release from the DO100% microgel ($R_{GDGE/polymer\,(w/w} = 0.025$) was measured as a function of pH and ionic strength. The protein release curves for pH 3, 4, 5 and 7 with an ionic strength of 0.05 M are displayed in Fig. 8A. The results show that the percentage of lysozyme release increased with decreasing pH, which was opposite to the trend of protein uptake. The protein release percentage was 50% at pH 3, 20% at pH 4 and nearly no protein release occurred at pH 5 and 7 after 5 h of equilibrium in the buffer. This suggests that the binding strength is stronger at high pH than at low pH. At low pH, even lysozyme molecules are strongly positively charged, but the microgel is weakly charged (the pK_a of COO^- on the microgel is around pH 3.5). A smaller amount of protein may be sufficient to compensate for few charges on the microgel. Therefore, extra lysozyme molecules will be dissociated from weakly charged microgels at low pH. However, at high pH, the microgel is strongly charged and proteins are weakly charged, as shown in Fig. 7A. Thus, protein uptake at saturation was the highest at high pH since more proteins were needed to compensate for the strong charges on the microgel. This indicates that the binding strength is quite high at pH 7. Thus, nearly no proteins were released from the microgel in the buffer at pH 7. For oxidized starch microgel cross-linked with STMP, we find that the binding strength between gel and lysozyme is strong at low pH rather than high pH. It might due to charge regulation which played a role in protein absorption for STMP cross-linked microgel (Li et al., 2010). Fig. 8B shows that the percentage of protein release increased with increasing ionic strength. There was a dramatic increase in protein release at an ionic strength of 0.5 M, as nearly all proteins were released after 5 h. 20% of proteins were released at an ionic strength of 0.2 M and nearly no proteins were released at ionic strengths of 0.05 M. This salt-triggered protein release occurred mainly due to the salt shielding effect on the electric double layer of the microgel and protein, which weakened the electrostatic interaction between them and led to protein release. We have established a model of protein release from STMP cross-linked starch microgels based on Fick's diffusion law by including the effective diffusion coefficient (D_{eff}) and the concentration ratio between free and bound proteins ($R_{free/bound}$) inside the microgel (Li et al., 2011a, 2011b). It was found that protein molecules absorbed inside the microgel are actually mobile, i.e. protein molecules dynamically attach and detach from binding sites inside the gel. Therefore, $R_{free/bound}$ was introduced in the model. It was concluded that increasing ionic strength increases the mobility of proteins and thus increases the concentration ratio between free and bound proteins, which leads to increased D_{eff} in the gel, thereby inducing a protein release. This may also explain why protein release was increased by increasing the ionic strength for GDGE cross-linked microgel.

4. Conclusion

We have prepared oxidized starch microgels which are capable of absorbing a large amount of lysozyme. The results provide insight into the factors that control the uptake and release of lysozyme by oxidized starch microgels. The DO100% microgel with a $R_{GDGE/polymer(w/w)}$ of 0.025 was considered to be the optimal gel type for protein absorption. The protein uptake at saturation (Γ_{sat}) was the highest at high pH and low ionic strength. We found that Γ_{sat} increased with increasing pH. This is because the protein binding capacity is mainly determined by charge compensation: with increasing pH, the positive charge on lysozyme decreases, while the negative charge on the microgel particle increases. Therefore, more protein molecules are required to neutralize for the charge on the gel and the binding capacity increases. The decreased Γ_{sat} with increased ionic strength was mainly due to the shielding effect on the electrostatic interaction between the gel and proteins caused by a high salt concentration. Protein release was triggered by decreasing the pH and/or increasing the ionic strength, since the binding strength was the lowest at low pH and high ionic strength. The results suggest that oxidized microgels can be potentially applied in the controlled uptake and release of proteins.

Acknowledgments

The financial support of the National Natural Science Foundation of China (NSFC 31201334, 31471577) and the Scientific Research Foundation for the Returned Overseas Chinese Scholars, State Education Ministry are gratefully acknowledged.

References

Bardajee, G. R., & Hooshyar, Z. (2013). A novel biocompatible magnetic iron oxide nanoparticles/hydrogel based on poly(acrylic acid) grafted onto starch for controlled drug release. *Journal of Polymer Research*, *20*(11).

Bysell, H., & Malmsten, M. (2006). Visualizing the interaction between poly-L-lysine and poly(acrylic acid) microgels using microscopy techniques: Effect of electrostatics and peptide size. *Langmuir*, *22*(12), 5476–5484.
Cai, C., Bakowsky, U., Rytting, E., Schaper, A. K., & Kissel, T. (2008). Charged nanoparticles as protein delivery systems: A feasibility study using lysozyme as model protein. *European Journal of Pharmaceutics and Biopharmaceutics*, *69*(1), 31–42.
Chen, X., Wang, S., Lu, M., Chen, Y., Zhao, L., Li, W., et al. (2014). Formation and characterization of light-responsive TEMPO-oxidized Konjac glucomannan microspheres. *Biomacromolecules*, *15*(6), 2166–2171.
Costa, D., Valente, A. J. M., Pais, A. A. C. C., Miguel, M. G., & Lindman, B. (2010). Cross-linked DNA gels: Disruption and release properties. *Colloids and Surfaces A: Physicochemical and Engineering Aspects*, *354*(1–3), 28–33.
de Nooy, A. E. J. (1997). *Selective oxidation of primary alcohol groups in polysaccharides* (Ph.D. thesis). Delft, The Netherlands: Technical University of Delft.
Drapala, P. W., Jiang, B., Chiu, Y. C., Mieler, W. F., Brey, E. M., Kang-Mieler, J. J., et al. (2014). The effect of glutathione as chain transfer agent in PNIPAAm-based thermo-responsive hydrogels for controlled release of proteins. *Pharmaceutical Research*, *31*(3), 742–753.
Eichenbaum, G. M., Kiser, P. F., Dobrynin, A. V., Simon, S. A., & Needham, D. (1999). Investigation of the swelling response and loading of ionic microgels with drugs and proteins: The dependence on cross-link density. *Macromolecules*, *32*(15), 4867–4878.
Fleisher, H. C., & Vigh, G. (2005). Hydrolytically stable, diaminocarboxylic acid-based membranes buffering in the pH range from 6 to 8.5 for isoelectric trapping separations. *Electrophoresis*, *26*(13), 2511–2519.
Gonzalez, J. S., Nicolás, P., Ferreira, M. L., Avena, M., Lassalle, V. L., & Alvarez, V. A. (2014). Fabrication of ferrogels using different magnetic nanoparticles and their performance on protein adsorption. *Polymer International*, *63*(2), 258–265.
Grznarova, G., Yu, S., Stefuca, V., & Polakovic, M. (2005). Quantitative characterization of pore structure of cellulose gels with or without bound protein ligand. *Journal of Chromatography A*, *1092*(1), 107–113.
Guilherme, M. R., Oliveira, R. S., Mauricio, M. R., Cellet, T. S. P., Pereira, G. M., Kunita, M. H., et al. (2012). Albumin release from a brain-resembling superabsorbent magnetic hydrogel based on starch. *Soft Matter*, *8*(24), 6629.
Hosseininasab, S., Pashaei-Asl, R., Khandaghi, A. A., Nasrabadi, H. T., Nejati-Koshki, K., Akbarzadeh, A., et al. (2014). Synthesis, characterization, and in vitro studies of PLGA-PEG nanoparticles for oral insulin delivery. *Chemical Biology & Drug Design*, *84*(3), 307–315.
Imren, D., Gümüsderelioglu, M. E., & Güner, A. (2010). In vitro release kinetics of bovine serum albumin from highly swellable dextran hydrogels. *Journal of Applied Polymer Science*, *115*(2), 740–747.
Koetting, M. C., & Peppas, N. A. (2014). pH-Responsive poly(itaconic acid-co-N-vinylpyrrolidone) hydrogels with reduced ionic strength loading solutions offer improved oral delivery potential for high isoelectric point-exhibiting therapeutic proteins. *International Journal of Pharmaceutics*, *471*(1–2), 83–91.
Lack, S., Dulong, V., Le Cerf, D., Picton, L., Argillier, J. F., & Muller, G. (2004). Hydrogels based on pullulan crosslinked with sodium trimetaphosphate (STMP): Rheological study. *Polymer Bulletin*, *52*(6), 429–436.
Lau, T. T., & Wang, D. A. (2013). Bioresponsive hydrogel scaffolding systems for 3D constructions in tissue engineering and regenerative medicine. *Nanomedicine*, *8*(4), 655–668.
Li, Y., de Vries, R., Kleijn, M., Slaghek, T., Timmermans, J., Stuart, M. C., et al. (2010). Lysozyme uptake by oxidized starch polymer microgels. *Biomacromolecules*, *11*(7), 1754–1762.
Li, Y., de Vries, R., Slaghek, T., Timmermans, J., Cohen Stuart, M. A., & Norde, W. (2009). Preparation and characterization of oxidized starch polymer microgels for encapsulation and controlled release of functional ingredients. *Biomacromolecules*, *10*(7), 1931–1938.
Li, Y., Kleijn, J. M., Stuart, M. A. C., Slaghek, T., Timmermans, J., & Norde, W. (2011). Mobility of lysozyme inside oxidized starch polymer microgels. *Soft Matter*, *7*(5), 1926–1935.
Li, Y., Norde, W., & Kleijn, J. M. (2012). Stabilization of protein-loaded starch microgel by polyelectrolytes. *Langmuir*, *28*(2), 1545–1551.
Li, X., Wang, Y., Chen, J., Wang, Y., Ma, J., & Wu, G. (2014). Controlled release of protein from biodegradable multi-sensitive injectable poly(ether-urethane) hydrogel. *ACS Applied Materials and Interfaces*, *6*(5), 3640–3647.
Li, Y., Zhang, Z., van Leeuwen, H. P., Stuart, M. A. C., Norde, W., & Kleijn, J. M. (2011). Uptake and release kinetics of lysozyme in and from an oxidized starch polymer microgel. *Soft Matter*, *7*(21), 10377–10385.
Liu, L., Zhai, J., Zhu, C., Gao, Y., Wang, Y., Han, Y., et al. (2015). One-pot synthesis of 3-dimensional reduced graphene oxide-based hydrogel as support for microbe immobilization and BOD biosensor preparation. *Biosensors & Bioelectronics*, *63*, 483–489.
Lynam, D., Peterson, C., Maloney, R., Shahriari, D., Garrison, A., Saleh, S., et al. (2014). Augmenting protein release from layer-by-layer functionalized agarose hydrogels. *Carbohydrate Polymers*, *103*, 377–384.
Mehyar, G. F., Liu, Z., & Han, J. H. (2008). Dynamics of antimicrobial hydrogels in physiological saline. *Carbohydrate Polymers*, *74*(1), 92–98.
Qu, J.-B., Huan, G.-S., Chen, Y.-L., Zhou, W.-Q., Liu, J.-G., & Huang, F. (2014). Coating gigaporous polystyrene microspheres with cross-linked poly(vinyl alcohol) hydrogel as a rapid protein chromatography matrix. *ACS Applied Materials and Interfaces*, *6*(15), 12752–12760.
Saunders, B. R., & Vincent, B. (1999). Microgel particles as model colloids: Theory, properties and applications. *Advances in Colloid and Interface Science*, *80*(1), 1–25.
Schesny, M. K., Monaghan, M., Bindermann, A. H., Freund, D., Seifert, M., Eble, J. A., et al. (2014). Preserved bioactivity and tunable release of a SDF1-GPVI bispecific protein using photo-crosslinked PEGda hydrogels. *Biomaterials*, *35*(25), 7180–7187.
Shahbuddin, M., MacNeil, S., & Rimmer, S. (2012). Synthesis and preparation of konjac glucomannan hydrogel for wound healing. *Journal of Tissue Engineering and Regenerative Medicine*, *6*, 186–187.
Singh, B., Bala, R., & Chauhan, N. (2008). In vitro release dynamics of model drugs from psyllium and acrylic acid based hydrogels for the use in colon specific drug delivery. *Journal of Materials Science Materials in Medicine*, *19*(8), 2771–2780.
Spagnol, C., Rodrigues, F. H. A., Pereira, A. G. B., Fajardo, A. R., Rubira, A. F., & Muniz, E. C. (2012). Superabsorbent hydrogel nanocomposites based on starch-g-poly(sodium acrylate) matrix filled with cellulose nanowhiskers. *Cellulose*, *19*(4), 1225–1237.
Tomic, K., Veeman, W. S., Boerakker, M., Litvinov, V. M., & Dias, A. A. (2008). Lateral and rotational mobility of some drug molecules in a poly(ethylene glycol) diacrylate hydrogel and the effect of drug-cyclodextrin complexation. *Journal of Pharmaceutical Sciences*, *97*(8), 3245–3256.
Wang, Z., Li, Y., Chen, L., Xin, X., & Yuan, Q. (2013). A study of controlled uptake and release of anthocyanins by oxidized starch microgels. *Journal of Agricultural and Food Chemistry*, *61*(24), 5880–5887.
Widjaja, L. K., Bora, M., Chan, P. N. P. H., Lipik, V., Wong, T. T. L., & Venkatraman, S. S. (2014). Hyaluronic acid-based nanocomposite hydrogels for ocular drug delivery applications. *Journal of Biomedical Materials Research A*, *102*(9), 3056–3065.
Zamora-Mora, V., Velasco, D., Hernandez, R., Mijangos, C., & Kumacheva, E. (2014). Chitosan/agarose hydrogels: Cooperative properties and microfluidic preparation. *Carbohydrate Polymers*, *111*, 348–355.